

One-dimensional magnonic crystal as a medium with magnetically tunable disorder on a periodical lattice

J. Ding¹, M. Kostylev², and A. O. Adeyeye¹

¹*Information Storage Materials Laboratory, Department of Electrical and Computer Engineering, National University of Singapore, Singapore 117576 and*

²*School of Physics, University of Western Australia, Crawley, Western Australia 6009, Australia*
(Dated: November 9, 2018)

We show that periodic magnetic nanostructures (magnonic crystals) represent an ideal system for studying excitations on disordered periodical lattices because of the possibility of controlled variation of the degree of disorder by varying the applied magnetic field. Ferromagnetic resonance (FMR) data collected inside minor hysteresis loops for a periodic array of Permalloy nanowires of alternating width and magnetic force microscopy images of the array taken after running each of these loops were used to establish convincing evidence that there is a strong correlation between the type of FMR response and the degree of disorder of the magnetic ground state. We found two types of dynamic responses: anti-ferromagnetic (AFM) and ferromagnetic (FM), which represent collective spin wave modes or collective magnonic states. Depending on the history of sample magnetization either AFM or FM state is either the fundamental FMR mode or represents a state of a magnetic defect on the artificial crystal. A fundamental state can be transformed into a defect one and vice versa by controlled magnetization of the sample.

PACS numbers: 75.75.-c, 75.30.Ds, 75.78.-n, 78.67.Pt

Arrays of magnetic nanowires (NW) have generated considerable scientific interest due to their potential application for microwave devices [1, 2] and domain wall logic [3]. On the other hand they represent a variety of artificial crystals [4] in which wave excitations can propagate. Magnetic artificial crystals are called magnonic crystals (MC), the wave excitations of which are collective spin wave (magnonic) modes which exist in the microwave frequency range [6–10]. In contrast to photonic [4] and sonic [5] crystals magnonic crystals are easily frequency tunable by applying magnetic field to the structure. MC response at remanence currently attracts a lot of attention ([10–13]). First, minimizing the bias magnetic field applied to a nanostructure is important for possible applications in tunable microwave devices. Second, magnetic periodic nanostructures may have a number of periodic magnetic configurations (magnetic ground states) for the same periodic geometry of the material, and the material can be switched between these ground states. Controlling of the magnonic frequency gap by switching between two ground states [10] and reconfiguration of a magnonic crystals has been recently demonstrated ([11, 12]). Importantly, in these previous experimental studies additional microwave responses were seen within the hysteresis loops which are not present in the theories which assume a perfect magnetic periodic order for the array [10, 11]. It was supposed that these branches originate from *magnetic* disorder on the periodic lattice. In the present paper we will experimentally show that these branches indeed originate from deviation from a perfect magnetic periodic order. This deviation takes the form of "magnetic defects" which represent individual wires or small clusters of wires in which magnetization vector points in a wrong direction with respect

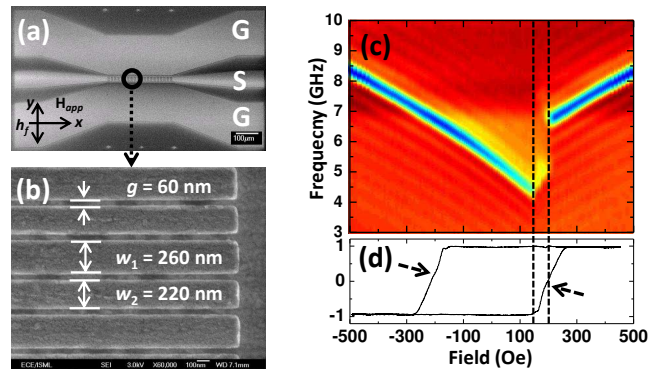


FIG. 1: (Color Online): (a): SEM image of the CPW showing the ground - signal - ground (G-S-G) lines. (b): SEM image of the alternating widths nanowires array ($w_1 = 260$ nm, $w_2 = 220$ nm and edge-to-edge separation $g = 60$ nm). (c): Full loop 2D FMR absorption spectra for the NW arrays. (d): Normalized M-H loop for the array.

to the average magnetic order of MC.

Defects on a crystal lattice are objects of fundamental importance: this can result on weak localization of electron on a crystal lattice in a condensed matter [14]; Anderson localization can occur due to disorder in different systems, such as condensed matter [15], Bose-Einstein Condensate [16], and photonic crystals [17, 18] (see also extensive literature in all those papers). Importantly, to study the effects of disorder and defects on a crystal lattice is not simple. Often one has to fabricate a large number of samples with different degrees of disorder, but otherwise identical, like it was recently done in Ref.[14].

In this paper we investigate the effect of magnetic disorder on magnonic excitations on the lattice of a 1D

MC in the form of a dipole coupled array of magnetic nanowires [7]. We demonstrate that this material represents an excellent model system for studying disorder because of the possibility of controlled variation of disorder degree by varying a magnetic field applied to the sample.

Array of densely packed $\text{Ni}_{80}\text{Fe}_{20}$ NWs was fabricated directly on top of a coplanar waveguide (CPW) using electron beam lithography, E-beam evaporation and lift off processing. Figs.1(a-b) shows the SEM images of the CPW and two periods of alternating width NWs. The X, Y and Z (out-of-plane) axes of a Cartesian frame of reference are parallel to the length $l=10\ \mu\text{m}$, width w and thickness $t=30\ \text{nm}$ of NWs, respectively. Each period consists of two NWs with different widths $w_1=260\ \text{nm}$ and $w_2=220\ \text{nm}$. The edge-to-edge spacing w_g is $60\ \text{nm}$. Thus, the structure period is $w_a=w_1+w_2+2w_g=600\ \text{nm}$. The array size in the direction of the array periodicity is $20\ \mu\text{m}$. The magnetic ground state of NW arrays was characterized using a magneto-optical Kerr effect magnetometer (MOKE) with a laser spot size of about $10\ \mu\text{m}$ and by magnetic force microscopy (MFM). The FMR responses were measured in the $1-20\ \text{GHz}$ range using a microwave vector network analyzer (VNA) Agilent 8363C. To obtain a high frequency response, VNA is connected to CPW by a ground-signal-ground (GSG)-type microwave probe similar to that reported in Ref. [10]. The magnetic radio-frequency field h_f of CPW is applied along the Y direction, while an external static magnetic field (H_{app}) is along the X direction as shown in Fig.1(a). FMR measurements were performed at room temperature by sweeping the frequency for fixed H_{app} . This was repeated for a number of minor hysteresis loops for the sample. Each time we started from the negative saturation field $-H_{sat}=-500\ \text{Oe}$, passed through zero, and then gradually increased the field to a maximum $H_{max}<H_{sat}$ (forward half of a loop). The field is then subsequently decreased to $-H_{sat}$ (backward half of a loop). A number of minor loops with different values of H_{max} were run. At the end of each loop an MFM image of the remanent state was also taken after the H_{app} had been increased again from $-H_{sat}$ to the same H_{max} and then switched off to achieve the remnant state.

Fig.1(c) displays the absorption spectra for the major hysteresis loop for the sample (H_{app} ranges from $-500\ \text{Oe}$ to $+500\ \text{Oe}$ which corresponds to the forward half of the loop). A stepwise increase in the resonance frequency is seen in the panels between 140 and $210\ \text{Oe}$ and can be attributed to the reversal of magnetization in the wider wires [11]. A magnetic ground state which is characterized by alignment of the static magnetization vector with H_{app} for the wider stripes and the counter-alignment of them for the narrower stripes ("Antiferromagnetic" (AFM) ground state) is expected for this field range. The normalized MOKE data shown in Fig.1(d) are in agreement with this type of the ground state. From

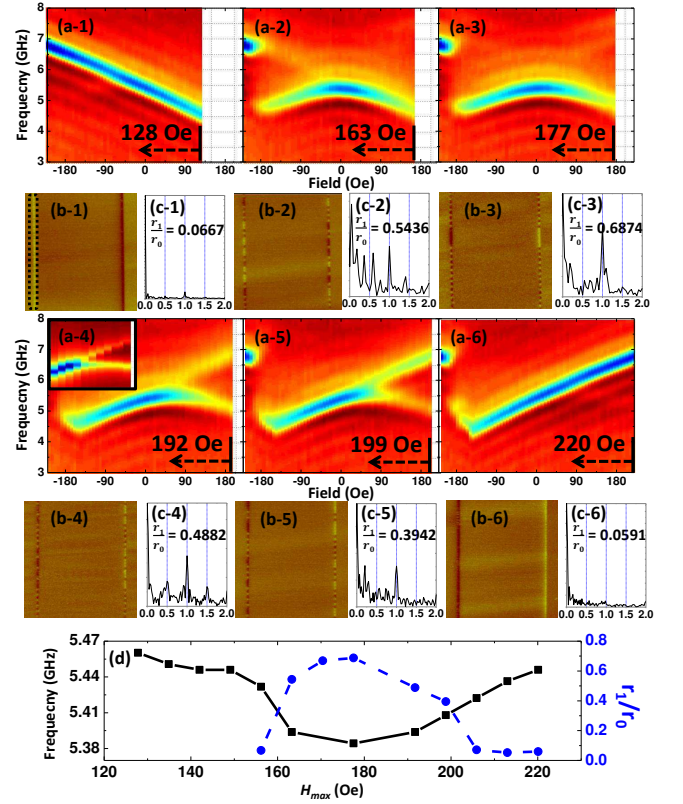


FIG. 2: (Color Online): (a-1) to (a-6): FMR absorption spectra inside the minor loops with $H_{max} = 128\ \text{Oe}$, $163\ \text{Oe}$, $177\ \text{Oe}$, $192\ \text{Oe}$, $199\ \text{Oe}$ and $220\ \text{Oe}$. (b-1) to (b-6): MFM images for the same H_{max} at remanence. (c-1) to (c-6): Fourier transforms of the respective MFM data. (d) Frequency of the fundamental mode at remanence (solid line) and the ratio r_0/r_1 (dashed line) as a function of H_{max} .

this panel one sees that the slope of the hysteresis loop slightly changes around $H_{app} = 170\ \text{Oe}$ (indicated by the dashed arrows) which evidences transition to the AFM state. Importantly, we do not see formation of a plateau, which was observed in the hysteresis loops in Ref. [19] (Figs.3 and 4 in that paper). This suggests the AFM state is not stabilized for a range of applied fields in the present case of small values for Δw and g . Rather, in agreement with a small squareness of the hysteresis loop in Fig.1(d) a gradual transition from a ferromagnetic (FM) ground state through an AFM one to a new FM state is expected.

In Figs.2(a-1) to (a-6), we show the FMR absorption spectra within the minor loops (H_{app} ranges from $-500\ \text{Oe}$ to H_{max} , with $128\ \text{Oe} \leq H_{max} \leq 220\ \text{Oe}$ for different loops). For clarity, only the backward half of the loop, for which H_{app} decreases from H_{max} to $-H_{sat}$, is shown. The forward halves of the loops are trivial: each of them coincides with the section $H_{app} \leq H_{max}$ of the spectrum in Fig.1(c) for the respective value of H_{max} .

Panels b-1 to b-6 of Fig.2 display the corresponding MFM images taken at remanence. The wires are oriented

horizontally. Two vertical lines close to the image edges with a contrast different from the rest of the area ("edge contrast lines") are signatures of the wire edges. A bright spot is consistent with the static magnetization vector pointing away from the spot and the dark spot is for the tip of magnetization vector pointing to the respective wire edge. First one observes that for each bright/dark spot at one edge of the array there is a respective spot of the opposite contrast (dark/bright) at the opposite edge. This fact together with an absence of signatures of stray fields of domain walls inside the array evidences that all the wires are in a monodomain state in all panels.

The degree of magnetic disorder varies between the panels. We quantify the disorder degree by performing a Fourier transform of the distribution of the MFM contrast along one of the edge contrast lines. Panels c-1 to c-6 display the Fourier spectra along with the ratio of the amplitudes r_1/r_0 of two important Fourier harmonics. One (r_1) corresponds to the Fourier wavenumber k_1 equal to the lattice vector $G=2\pi/(w_1 + w_2 + 2g)$, and the other (r_0) to the zero wavenumber $k = 0$. One sees that the richest spectrum displaying a largest number of harmonics for $k/G < 1$ is in Panel c-2. Indeed, the edge contrast for this state is the most irregular. Additional harmonics but of smaller relative amplitudes than in panel c-2 are also seen in Panels c-4 and c-5. They correspond to $k = G/2, k = G/3$, and $G/4$. By comparing these data with the respective MFM images one finds that the ground states are more regular in these cases. Panel c-3 displays just two prominent peaks for $k = 0$ and for $k = G$ and is characterized by the maximum value of r_1/r_0 (see Fig.2(d)). The Fourier peak at $k/G = 1$ corresponds to the AFM order. Indeed, the respective MFM image displays an almost perfect AFM order.

Let us first concentrate on the FMR response in Panels 2(a-1) and 2(a-6). Panel 2(a-1) is characterized by a single monotonically falling branch ($\omega(H_{app})$). The respective MFM image shows that this response originates from a ground state with a perfect ferromagnetic order with the static magnetization vector pointing to the right (Fig.2(b-1)). Similarly, the growing branch in Fig.2(a-6) existing for $\omega(H_{app})$ for $H_{app} > -120\text{Oe}$ is identified as a FMR response of the perfectly ferromagnetic ground state with the static magnetization vector points to the left (Fig.2(b-6)). This identification is in agreement with the theory of collective modes for the FM state [10, 11].

Let us now discuss Panels 2(a-3) and 2(b-3). The (H_{app}) curve for this minor loop is non-monotonic. In Ref. [10] this branch has been identified as the fundamental acoustic collective mode for the anti-ferromagnetic state. From Fig.2(b-3) one sees that, indeed, the ground state for this minor hysteresis loop is antiferromagnetic. This represents an experimental evidence for the previous identification [10] which was based solely on the theory. The experimentally observed state is actually not perfectly AFM, a 3-period long ferromagnetic defect is

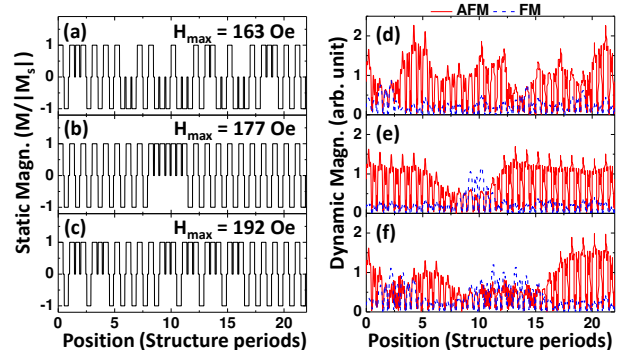


FIG. 3: (Color Online): (a-c): The magnetic ground states for $H_{max} = 163 \text{ Oe}$, 177 Oe and 192 Oe , respectively. (d-f): the respective calculated profiles of dynamic magnetization. Red solid line: AFM mode; blue dashed line: FM mode.

observed in the middle of the MFM image. This suggests that a faint response existing for $H_{app} > 0$ and monotonically growing in frequency with H_{app} may be the dynamic response of the FM defect.

Later we will confirm this conclusion by a numerical simulation. But first let us discuss the responses for the states which are transitional between the well ordered FM and the AFM states (Figs.2(a-2), 2(a-4) and 2(a-5)). The main observations which can be drawn from these panels are as follows. (i) The FMR response for the transitional states looks like combination of the responses for the FM and the AFM states in Figs.2(a-1), 2(a-6) and 2(a-3), such that the respective branches can be termed "FM" and "AFM" branches. (ii) Linewidths for the observed resonance peaks do not vary noticeably with H_{app} across each minor loop and between the loops and are very close to the linewidth obtained on a reference continuous film (the full linewidth is 0.5GHz). (iii) The shape of the AFM branch and the mode frequency at remanence varies between the loops (Fig.2(d)) and is correlated to r_1/r_0 .

In order to explain these features numerical simulations based on a 1D version of the model from [20] have been performed. The ground states for the linear dynamics simulations were assumed to be the same as observed in the respective MFM images (Figs.2(b-1) to (b-6)). To this end the experimental contrast line data were digitized such that +1 corresponds to static magnetization vector pointing to the right and -1 to one pointing to the left (Fig.3(a-c)). Periodic boundary conditions (PBC) at both ends of the digitized contrast lines were assumed. In the dynamic calculations using this ground state model we utilized the values for the saturation magnetization and for the resonance linewidths extracted from the FMR data obtained on a non-nanostructured reference sample.

An example of the results of simulation of a frequency vs. applied field dependencies is shown as an inset to Fig.2(a-4). One sees a good qualitative agreement with

the experiment. The simulated mode profiles for the disordered state are complicated (Fig.3). The simplest ones are observed for the ground state of Fig.2(b-3). As seen from Fig.3(b), the AFM ground state contains an FM defect which is 3 structure periods long. Accordingly, one observes one extended dynamic state of AFM nature (Fig.3(e)) whose amplitude noticeably decreases on the FM defect. This mode is responsible for the main peak of the FMR response. The defect has its own mode. Localization of the defect mode on the defect is relatively strong: the amplitude of the mode half a way between two neighboring defects (recall PBC) is about 20% of the maximum inside the defect. For this reason the FMR response of this mode is weak, and is consistent with a faint FM-type response seen in Fig.2(a-3). It is appropriate to term this weak response as an "impurity" or "defect" state of MC.

The ground state in Fig.3(a) (corresponds to Fig.2(b-2)) can be characterized as an AFM one with multiple single-site FM defects. From Fig.3(d) one sees that the dominating mode is the lower-frequency AFM mode. The higher-frequency FM modes has considerably smaller excitation amplitude which is in full agreement with Fig.2(a-2). Both modes are more extended than in Fig.3(e) and the picture shows less regularity, but still localization of particular modes on particular clusters, FM or AFM ones, is clearly seen. Again, one can characterize the FM mode as an impurity state based on the above considerations.

The ground state in Fig.3(c) (corresponds to Fig.2(b-4)) can be regarded as two defectless AFM clusters (4th-9th periods and from 16th period onwards) and two FM clusters (2-4) and (9-15) each having a number of single-site AFM defects (1 and 3 defects respectively). As in Fig.3(d) one observes that a small number of defects does not prohibit formation of a fundamental collective mode, in this case of one of the FM type. Both AF and defect-containing FM dynamic states are again extended, with a noticeable amplitude on the clusters of the different type. The excitation amplitudes of these two modes are comparable which is in agreement with the experimental data in Fig.2(a-4). This case clearly demonstrates potential of the wire arrays as a model medium for studying effects of disorder: a simple magnetization procedure transforms a state of AFM type with FM impurities (Fig.3(d)) into a state of FM type with AFM impurities.

Our simulation has also shown that mode frequencies for the transitional states noticeably deviate from ones for the respective frequencies for the array in the perfect FM and AFM states. This is in agreement with the experimental data in Fig.2(d), where variation of frequency of the main peak at remanence is shown as a function of H_{max} for the respective loop. In particular, considering a single FM cluster of the type in Fig.3b inside an AFM array in the simulation we found that the frequency of a mode localized on the cluster tends to the frequency

for an infinite array with the FM order with increase of the defect length. This suggests that the observed variation in frequency is due to an effect of confinement of the cluster inside the array (similar to confinement effect for a single wire [21]) and of its interaction with the AFM environment. The same applies to the fundamental (AFM) mode: its frequency is the smallest when no defect is present and increases due to confinement (recall PBC) as the FM defect grows.

In conclusion, we studied magnetic disorder on the arrays of dipole coupled nanowires. We found experimental evidence that switching of nanowires produces a disordered magnetic ground state inside the hysteresis loop. Collective dynamic states localized on clusters with different magnetic orders are formed and the respective FMR response inside the hysteresis loop represents a doublet, whereas outside the loop the fundamental oscillation is a FM singlet. Depending on the magnetization history either AFM or FM state of the doublet can be either a fundamental or a defect ("impurity") one. Localization of these dynamic states on the respective clusters is not very strong, the states extend into the clusters of different order such that their amplitude is noticeable everywhere. Individual magnetic defects inside the clusters do not prohibit formation of collective modes.

Acknowledgment: we acknowledge financial support from the National Research Foundation, Singapore under Grant No. NRF-G-CRP 2007-05, and from the Australian Research Council.

-
- [1] S. Choi *et al.*, Phys. Rev. Lett. **98**, 087205 (2007)
 - [2] H. Zhang *et al.*, Appl. Phys. Lett. **95**, 232503 (2009)
 - [3] X. Zhu *et al.*, Appl. Phys. Lett. **87**, 062503 (2005)
 - [4] E. Yablonovich *et al.*, J. Opt. Soc. Am. B, **10**, 283 (1993).
 - [5] T. Miyashita, Meas. Sci. Technol. **16** R47(2005)
 - [6] S. A. Nikitov *et al.*, J. Magn. Magn. Mater. **236** 320 (2001).
 - [7] G. Gubbiotti *et al.*, J. Phys. D: Appl. Phys. **43** 264003 (2010).
 - [8] S. Neusser *et al.*, Adv. Mater. **21**, 2927 (2009).
 - [9] V.V. Kruglyak *et al.*, Phys. Rev. Lett. **104**, 027201 (2010)
 - [10] J. Topp *et al.*, Phys. Rev. Lett. **104**, 207205 (2010)
 - [11] S. Tacchi *et al.*, Phys. Rev. B **82**, 184408 (2010)
 - [12] R. Zivieri, F. Montoncello, L. Giovannini, et al., "Collective spin modes in chains of dipolarly interacting rectangular magnetic dots", in print in Phys. Rev. B.
 - [13] A. Barman *et al.*, J. Phys. D: Appl. Phys. **43** 422001 (2010).
 - [14] Y. Niimi *et al.*, Phys. Rev. Lett. **102** 226801 (2009).
 - [15] P. W. Anderson, Phys. Rev. **109** 1492 (1958).
 - [16] J. Billy *et al.*, Nature, **453**, 81 (2008).
 - [17] S. John, Phys. Rev. Lett. **58** 2486 (1987).
 - [18] Y. Lahini *et al.*, Phys. Rev. Lett. **100**, 013906 (2008).
 - [19] S. Goolaup *et al.*, Phys. Rev. B **75**, 144430 (2007).
 - [20] S. Tacchi *et al.*, Phys. Rev. B, **82**, 024401 (2010).
 - [21] K. Yu. Guslienko *et al.*, Phys. Rev. B, **66**, 132402 (2002).